Supporting Information for:

Mutations alter RNA-mediated conversion of human prions

By: Erik J. Alred[1], Izra Lodangco[1], Jennifer Gallaher[1], Ulrich H.E. Hansmann*[1]

[1] University of Oklahoma, Department of Chemistry, 101 Stephenson Parkway, Norman, OK 73019-5251, USA

Contents

Attached Files

Atomic coordinates of start configurations for the 129M-178D wild type, 129V-178D wild type, 129M-178N mutant and 179V-178N mutant are available in PDB-format as separate files 129M178D.pdb, 129V178D.pdb, 129M178D.pdb and 129V178N.pdb.

Methods

Atomic coordinates of the start configurations of the four systems (129M-178D wild type, 129V-178D wild type, 129M-178N mutant and 179V-178N mutant) are available in PDB-format as separate files 129M178D.pdb,129V178D.pdb, 129M178D.pdb and 129V178N.pdb.

Results

Figures S1 – S3. Contact map of prion sequences

In order to emphasize the shift in hydrogen bonding and the corresponding structural rearrangements we show in **Figure S1** in the lower triangle the hydrogen bonding contact map for the 129M-178N mutant, in **Figure S2** the hydrogen bonding contact map for the 129V-178N mutants, and in **Figure S3** the hydrogen bonding contact map for the 129V-178D wild type variant. For comparison, we show in all three supplemental figures the corresponding contact map of the 129M-178D wild type (the topic of our previous study) in the upper triangle. For the three figures, we have measured the frequency of backbone-backbone hydrogen bonds in both docked and undocked structures, and color-coded the corresponding differences. If a given hydrogen bond is more commonly seen in the bound structure than in the unbound, the coloring is reddish, and greenish in the opposite case. Data are taken only from trajectories that started with configuration where the RNA fragment binds to the prion at either site 1 or site 3. With this coloring scheme we find, or instance, for the wild type 129M-178D for residues 140-161, which

are part of helix A, a loss of helical contacts marked by greenish coloring of point parallel to the diagonal, and a corresponding increase in contacts that suggest β arrangements marked by reddish points orthogonal to the diagonal. Similar unfolding of helix A, and additional unfolding is observed in the upper triangle of **S1** for the 129M-D178N mutant, and to a lesser degree in **S2** for the 129V-178N mutant. Note the weak signal for the 129V-178D wild type variant.

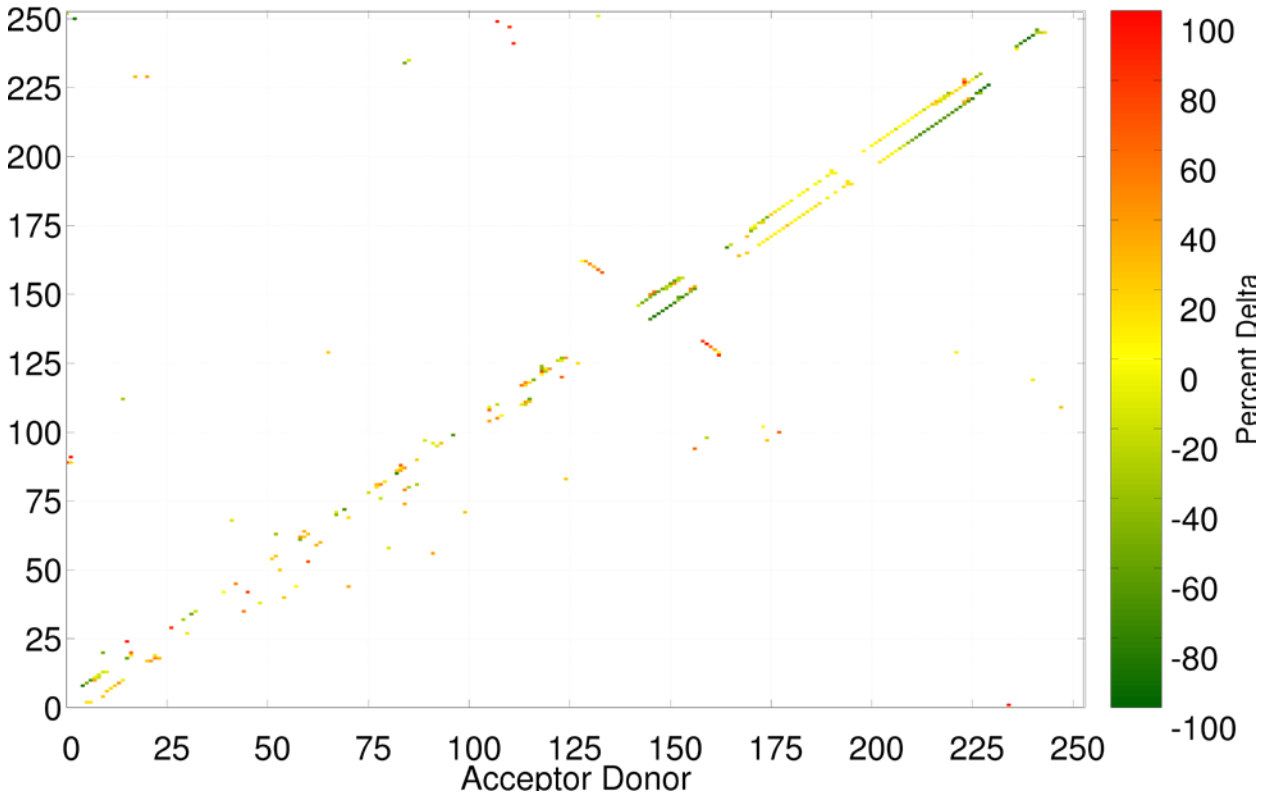

Figure S1: Difference in hydrogen bonding between bound and unbound prions for the 129M-178N mutant (below diagonal axis). For comparison, we show the corresponding frequency difference for the 129M-178D wild type (studied by us in previous work) in the upper triangle.

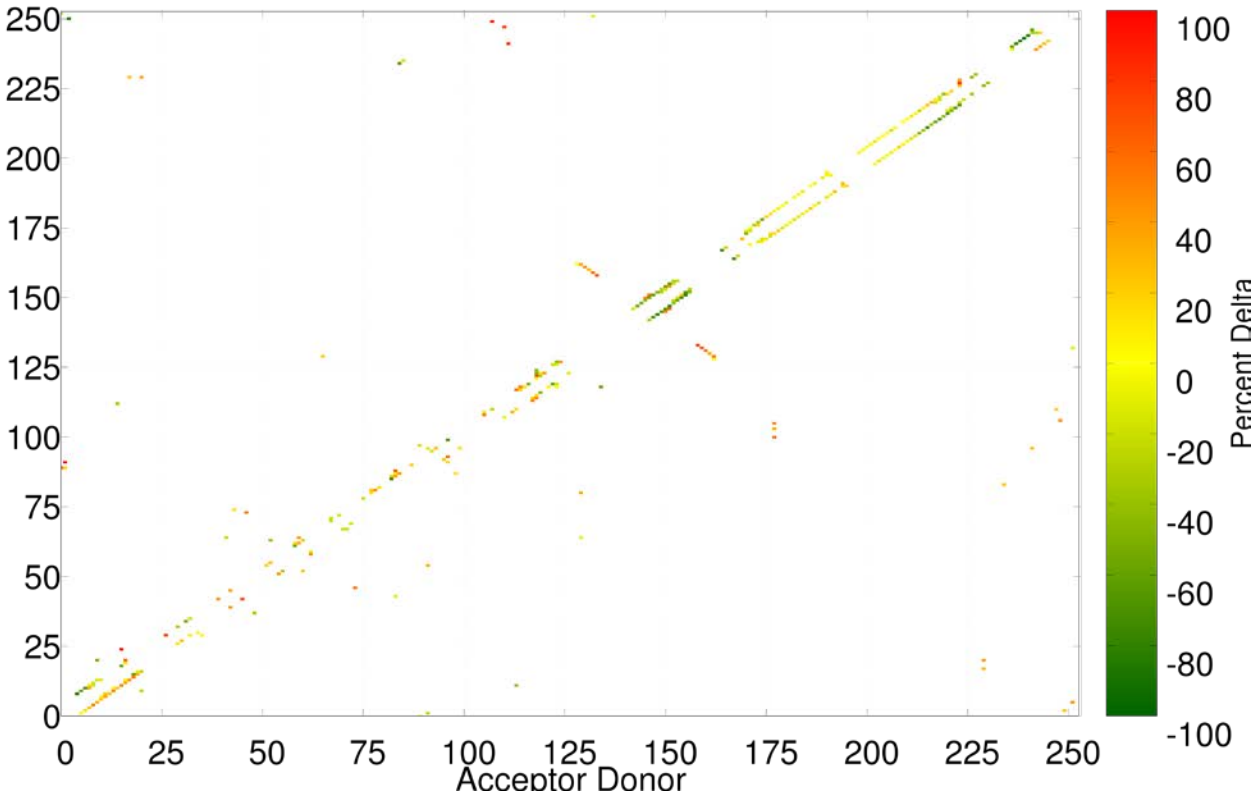

Figure S2: Difference in hydrogen bonding between bound and unbound prions for the 129V-178N mutant (below diagonal axis). For comparison, we show the corresponding frequency difference for the 129M-178D wild type (studied by us in previous work) in the upper triangle.

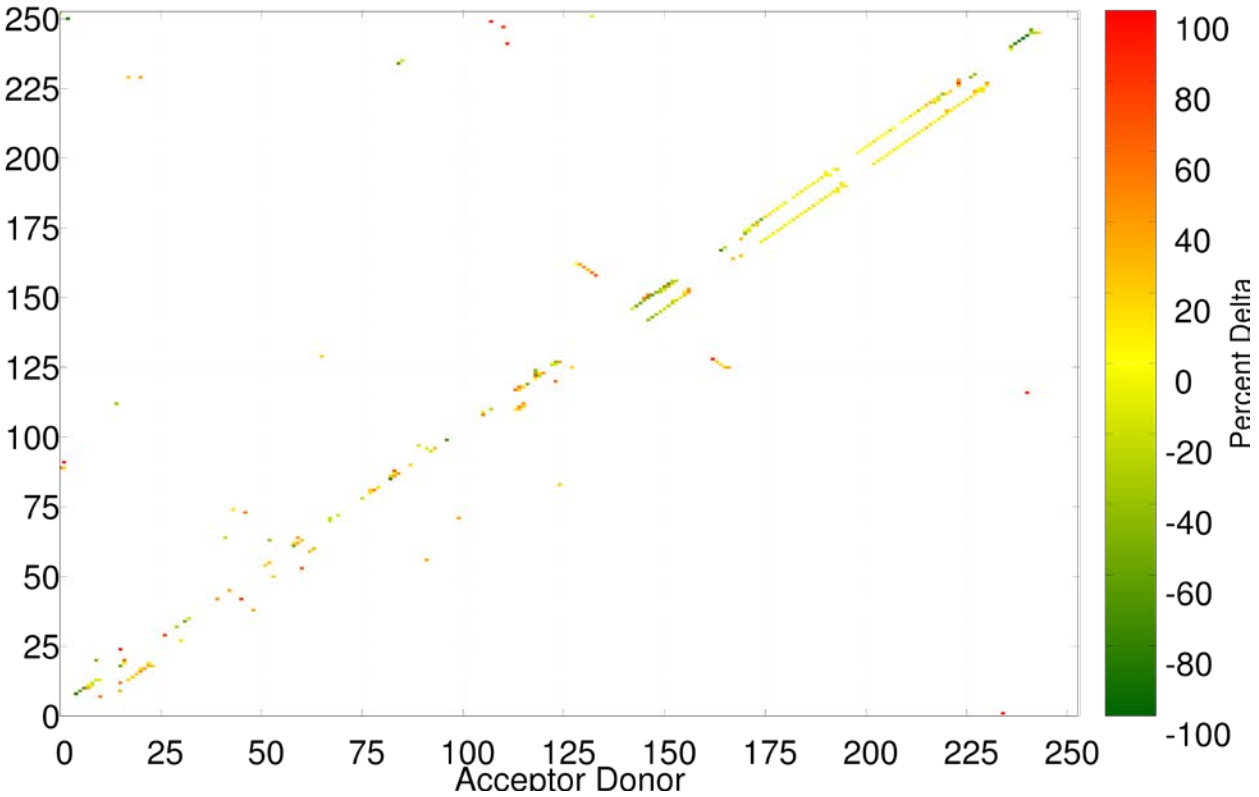

Figure S3: Difference in hydrogen bonding between bound and unbound prions for the 129V-178D wild type variant (below diagonal axis). For comparison, we show the corresponding frequency difference for the 129M-178D wild type (studied by us in previous work) in the upper triangle.

Tables S1 and S2: Helicity of helix A and helix C.

We list in **Table S1** the average probability of finding a 1-4 backbone hydrogen bonds in helix A for a given time period for all four systems. For comparison, we also show the corresponding frequencies for the undocked protein. Comparing the first 100ns with the last 100ns allows us to quantify the loss of helical hydrogen-bonding with time. **Table S2** shows the same quantities for helix C.

	129M-178D			129V-178D		
Backbone Hydrogen Bond	**Control 0 -300ns**	**Complex 0-100ns**	**Complex 200-300ns**	**Control 0-300ns**	**Complex 0-100ns**	**Complex 200-300ns**
V161-P157	50% (4%)	45% (5%)	10% (3%)	52% (3%)	51% (3%)	51% (4%)
V160-R156	75% (1%)	55% (3%)	16% (3%)	83% (3%)	78% (4%)	76% (5%)
Q159-H155	89% (4%)	62% (4%)	20% (4%)	90% (3%)	88% (4%)	80% (3%)
N158-M154	82% (4%)	65% (4%)	20% (4%)	81% (3%)	77% (4%)	79% (4%)
P157-N153	46% (4%)	43% (4%)	20% (4%)	47% (5%)	48% (3%)	53% (4%)
R156-E152	79% (2%)	66% (8%)	21% (4%)	82% (4%)	77% (5%)	79% (6%)
H155-R151	98% (4%)	81% (8%)	51% (3%)	96% (4%)	94% (7%)	86% (6%)
M154-Y150	74% (3%)	66% (7%)	31% (4%)	77% (4%)	79% (6%)	71% (5%)
N153-Y149	86% (4%)	50% (4%)	0% (0%)	89% (4%)	86% (5%)	92% (4%)
E152-R148	97% (2%)	72% (9%)	22% (4%)	96% (4%)	92% (6%)	89% (5%)
R151-D147	95% (3%)	41% (5%)	21% (4%)	93% (5%)	94% (5%)	84% (5%)
Y150-E146	99% (1%)	60% (5%)	10% (2%)	95% (4%)	95% (6%)	85% (6%)
Y149-W145	92% (5%)	41% (4%)	15.% (5%)	92% (4%)	85% (4%)	82% (4%)
R148-D144	76% (5%)	43% (6%)	23% (5%)	77% (3%)	66% (6%)	65% (4%)
D147-R143	97% (2%)	62% (5%)	26% (3%)	96% (4%)	95% (3%)	91% (4%)
	129M-178N			**129V-178N**		
V161-P157	52% (4%)	49% (2%)	16% (7%)	53% (4%)	53% (4%)	14% (3%)
V160-R156	80% (3%)	55% (4%)	15% (6%)	74% (4%)	62% (4%)	12% (6%)
Q159-H155	90% (4%)	67% (7%)	24% (8%)	88% (4%)	68% (5%)	22% (7%)
N158-M154	87% (6%)	69% (5%)	15% (8%)	81% (3%)	68% (4%)	18% (4%)
P157-N153	49% (7%)	49% (6%)	21% (5%)	47% (4%)	23% (4%)	16% (6%)
R156-E152	84% (5%)	67% (4%)	14% (7%)	78% (4%)	59% (8%)	19% (5%)
H155-R151	95% (3%)	40% (10%)	33% (6%)	97% (3%)	74% (9%)	29% (6%)
M154-Y150	70% (4%)	56% (9%)	20% (5%)	70% (8%)	53% (7%)	18% (4%)
N153-Y149	91% (3%)	49% (6%)	11% (7%)	85% (5%)	51% (9%)	11% (6%)
E152-R148	97% (3%)	48% (4%)	12% (5%)	95% (4%)	65% (8%)	16% (4%)
R151-D147	97% (2%)	36% (8%)	11% (8%)	96% (5%)	61% (7%)	14% (6%)
Y150-E146	92% (4%)	32% (5%)	14% (6%)	94% (3%)	65% (7%)	14% (7%)
Y149-W145	90% (5%)	47% (6%)	22% (6%)	95% (5%)	69% (6%)	16% (6%)
R148-D144	75% (4%)	39% (6%)	13% (7%)	80% (4%)	62% (7%)	10% (5%)
D147-R143	98% (2%)	42% (7%)	14% (6%)	94% (6%)	64% (8%)	12% (7%)

Table S1: Helical contacts in helix A. Data are for complexes where the RNA-fragment binds to either site 1 or site 3.

	129M-178D			129V-178D		
Backbone Hydrogen Bond	**Control 0 -300ns**	**Complex 0-100ns**	**Complex 200-300ns**	**Control 0-300ns**	**Complex 0-100ns**	**Complex 200-300ns**
Q227-Q223	36% (5%)	27% (6%)	25% (7%)	35% (5%)	27% (6%)	35% (5%)
Y226-S222	41% (5%)	40% (4%)	32% (4%)	39% (5%)	40% (5%)	30% (5%)
Y225-E221	59% (5%)	54% (3%)	69% (4%)	62% (7%)	58% (7%)	55% (6%)
A224-R220	66% (6%)	58% (6%)	71% (6%)	67% (6%)	69% (5%)	76% (7%)
Q223-E219	78% (5%)	79% (4%)	73% (5%)	74% (5%)	69% (6%)	65% (6%)
S222-Y218	91% (3%)	89% (4%)	96% (4%)	89% (4%)	88% (6%)	90% (6%)
E221-Q217	94% (4%)	94% (4%)	93% (4%)	92% (3%)	81% (7%)	97% (3%)
R220-T216	95% (3%)	85% (5%)	87% (5%)	97% (3%)	90% (5%)	86% (5%)
E219-I215	94% (5%)	85% (5%)	87% (6%)	92% (3%)	92% (4%)	90% (3%)
Y218-C214	89% (4%)	78% (7%)	98% (5%)	90% (4%)	87% (4%)	94% (5%)
Q217-M213	88% (4%)	85% (4%)	87% (5%)	92% (3%)	88% (5%)	91% (4%)
T216-Q212	88% (3%)	81% (5%)	93% (6%)	95% (3%)	87% (5%)	91% (4%)
I215-E211	87% (5%)	90% (4%)	94% (5%)	91% (3%)	94% (4%)	98% (5%)
C214-V210	79% (5%)	72% (4%)	81% (5%)	79% (5%)	66% (7%)	75% (7%)
M213V209	95% (4%)	89% (4%)	91% (5%)	90% (4%)	91% (4%)	97% (3%)
Q212-R208	92% (3%)	90% (5%)	98% (3%)	93% (2%)	84% (7%)	96% (5%)
E211-E207	73% (6%)	66% (6%)	74% (5%)	78% (6%)	82% (7%)	82% (6%)
V210-M206	88% (5%)	80% (6%)	85% (4%)	94% (4%)	83% (7%)	86% (5%)
V209-M205	79% (5%)	81% (5%)	84% (5%)	82% (3%)	85% (6%)	78% (7%)
R208-K204	92% (3%)	85% (6%)	86% (4%)	95% (3%)	86% (5%)	81% (5%)
E207-V203	93% (5%)	86% (4%)	96% (4%)	98% (3%)	94% (3%)	83% (5%)
M206-D202	97% (4%)	88% (5%)	87% (4%)	92% (3%)	90% (5%)	91% (4%)
M205-T201	70% (5%)	73% (5%)	76% (5%)	78% (5%)	76% (3%)	71% (7%)
K204-E200	91% (5%)	87% (6%)	83% (3%)	88% (5%)	82% (6%)	93% (3%)
	129M-178N			**129V-178N**		
Q227-Q223	29% (7%)	13% (9%)	10% (8%)	30% (5%)	22% (4%)	17% (6%)
Y226-S222	43% (6%)	29% (6%)	13% (7%)	31% (5%)	25% (5%)	11% (7%)
Y225-E221	72% (7%)	49% (8%)	12% (6%)	62% (7%)	58% (3%)	10% (8%)
A224-R220	63% (9%)	43% (7%)	15% (8%)	69% (6%)	69% (5%)	21% (9%)
Q223-E219	72% (6%)	46% (8%)	21% (7%)	79% (5%)	67% (5%)	17%(10%)
S222-Y218	88% (4%)	60% (5%)	24% (6%)	89% (4%)	75% (6%)	21% (8%)

E221-Q217	94% (7%)	51% (8%)	24% (7%)	84% (6%)	70% (6%)	14% (8%)
R220-T216	97% (4%)	67% (9%)	27% (9%)	94% (5%)	85% (5%)	33% (7%)
E219-I215	82% (5%)	64% (8%)	24% (6%)	92% (3%)	87% (4%)	15% (6%)
Y218-C214	92% (5%)	58% (7%)	26% (5%)	91% (4%)	76% (5%)	26% (8%)
Q217-M213	91% (4%)	62% (7%)	30% (4%)	87% (4%)	83% (4%)	40% (6%)
T216-Q212	93% (3%)	67% (6%)	41% (7%)	86% (4%)	72% (4%)	42% (7%)
I215-E211	84% (4%)	53% (8%)	38% (6%)	87% (4%)	76% (5%)	42% (5%)
C214-V210	81% (8%)	67% (5%)	37% (7%)	72% (6%)	59% (4%)	39% (6%)
M213V209	82% (4%)	61% (8%)	31% (5%)	98% (3%)	89% (5%)	26% (7%)
Q212-R208	93% (7%)	68% (6%)	27% (4%)	93% (5%)	97% (5%)	16% (8%)
E211-E207	87% (6%)	77% (6%)	31% (6%)	81% (5%)	77% (6%)	20% (7%)
V210-M206	95% (3%)	88% (8%)	55% (7%)	92% (4%)	82% (5%)	52% (7%)
V209-M205	83% (6%)	77% (5%)	44% (4%)	77% (5%)	72% (4%)	31% (8%)
R208-K204	92% (4%)	82% (9%)	53% (6%)	98% (5%)	95% (4%)	44% (7%)
E207-V203	94% (5%)	89% (6%)	87% (5%)	93% (5%)	95% (5%)	93% (6%)
M206-D202	92% (4%)	90% (5%)	87% (4%)	88% (4%)	79% (4%)	84% (7%)
M205-T201	73% (9%)	70% (6%)	72% (5%)	72% (4%)	60% (5%)	69% (5%)
K204-E200	83% (7%)	79% (4%)	88% (3%)	91% (4%)	83% (4%)	86% (8%)

Table S2: Helical contacts for helix C. Data are for complexes where the RNA-fragment binds to either site 1 or site 3.